JOURNAL OF APPLIED SCIENCE AND ENGINEERING MATERIALS

DFT AND HF STUDY OF STRUCTURAL, SPECTROSCOPİC, THERMOCHEMİCAL, AND ELECTRONİC PROPERTİES OF 2-ETHOXY-5-FLUORO-1H-PYRİMİDİN-4-ONE

2-ETHOXY-5-FLUORO-1H-PYRİMİDİN-4-ONE BİLEŞİĞİNİN YAPISAL, SPEKTROSKOPİK, TERMOKİMYASAL ve ELEKTRONİK ÖZELLİKLERİNİN DFT ve HF YÖNTEMLERİYLE İNCELENMESİ

Gülnur KURTUL
Dr, Bolu Abant İzzet Baysal University, https://ror.org/01x1kqx83, glnr85@gmail.com, 0000-0002-4497-6780
Ümit ERDEM
Assoc. Prof. Dr, Kırıkkale University, https://ror.org/01zhwwf82, umiterdem@kku.edu.tr, 0000-0002-0480-8176
Gürcan YILDIRIM
Prof. Dr, Bolu Abant İzzet Baysal University, https://ror.org/01x1kqx83, yildirim_g@ibu.edu.tr, 0000-0002-5177-3703
Mustafa Burak TÜRKOZ
Prof. Dr, Karabük University, ror.org/04wy7gp54, turkozmb@gmail.com, 0000-0002-4127-7650

Makale Türü:
Araştırma

Geliş Tarihi:

Revizyon Tarihi:

Kabul Tarihi:

DOI:

Bu makaleye atıf vermek için:

Özet

Yapısal, spektroskopik, termokimyasal, yük dağılımı ve elektronik özelliklerini aydınlatmak için, yoğunluk fonksiyonel teorisi (DFT) ve Hartree-Fock (HF) yöntemleri kullanılarak B3LYP/6-31+G(d,p) ve HF/6-31+G(d) seviyelerinde 2-ethoxy-5-fluoro-1H-pyrimidin-4-one ($C_6H_7FN_2O_2$) üzerinde kapsamlı bir kuantum-kimyasal inceleme gerçekleştirilmiştir. Optimize edilmiş geometri; pirimidinon halkasının, floro ikamesinin, karbonil grubunun ve etoksi grubunun moleküler elektronik yapıyı ortaklaşa yönettiği kararlı bir heterosiklik yapıyı ortaya koymaktadır. Hesaplanan geometrik parametreler teorik yaklaşımlar arasında iyi bir uyuma işaret ederek, optimize edilmiş moleküler modelin güvenilirliğini doğrulamaktadır. Teorik 1H ve 13C NMR kimyasal kaymaları GIAO yöntemi kullanılarak değerlendirilmiş ve CDCl3 içinde kaydedilen mevcut deneysel verilerle karşılaştırılmıştır. DFT hesaplamaları, deneysel kimyasal kaymaları HF yönteminden daha doğru bir şekilde yeniden üreterek, manyetik ekranlama sabitlerini tahmin etmede elektron korelasyon etkilerinin önemini vurgulamaktadır. Elektronegatif azot, oksijen ve flor atomlarına bağlı karbon atomlarında belirgin bir ekranlama kaybı (deshielding) gözlenirken, etoksi grubu karbonları ve hidrojen atomları nispeten daha düşük kimyasal kaymalar sergilemektedir. Atomik yük dağılımları ayrıca Mulliken popülasyonu ve atomik polar tensör (APT) şemaları kullanılarak analiz edilmiştir. Sonuçlar, molekül içinde belirgin bir elektronik polarizasyon olduğunu; karbonil oksijeni, flor atomu ve pirimidin azot atomlarının önemli ölçüde negatif yük yoğunlukları taşıdığını, buna karşılık çeşitli karbon ve hidrojen atomlarının pozitif yük birikimi sergilediğini ortaya koymaktadır. Ön moleküler orbital (FMO) analizi, HOMO'nun (En Yüksek İşgal Edilmiş Moleküler Orbital) ağırlıklı olarak pirimidinon halkası ve heteroatom bakımından zengin bölgelerde lokalize olduğunu, LUMO'nun (En Düşük Boş Moleküler Orbital) ise heterosiklik yapının karbonil ve flor içeren kısımlarında yoğunlaştığını göstermektedir. Bu uzamsal ayrım, molekül içi yük transfer süreçlerini kolaylaştırmaktadır. Elektronegatiflik, kimyasal sertlik, yumuşaklık, kimyasal potansiyel ve elektrofilisite indeksi dahil olmak üzere türetilmiş küresel reaktivite tanımlayıcıları ile birlikte HOMO-LUMO enerji aralığı, elektronik kararlılık ve kimyasal reaktivitenin dengeli bir kombinasyonuna işaret etmektedir. UV-Vis spektral analizi, elektronik soğurma davranışının, konjuge heterosiklik sistemi ve heteroatom ortaklanmamış elektron çiftlerini içeren $\pi \rightarrow \pi^*$ ve $n \rightarrow \pi^*$ geçişlerinin hakimiyetinde olduğunu ortaya koymaktadır. Ayrıca elektrostatik potansiyel (ESP) ve moleküler elektrostatik potansiyel (MEP) analizleri; karbonil oksijen atomunu, flor atomunu ve halka azot atomlarını en elektron yoğun bölgeler olarak tanımlarken, N-H ve etoksi hidrojen atomlarını temel pozitif potansiyel bölgelerini oluşturmaktadır. Sonuç olarak, elde edilen teorik sonuçlar 2-etoksi-5-flor-1H-pirimidin-4-on'un oldukça polarize bir elektronik yapıya, iyi tanımlanmış reaktif merkezlere ve elverişli yük transfer özelliklerine sahip olduğunu göstermektedir. Bulgular, yapısal kararlılığı, spektroskopik davranışı ve reaktivite kalıpları hakkında detaylı bir anlayış sağlamakta olup, farmasötik, tarım kimyasalı ve fonksiyonel malzeme alanlarındaki potansiyel önemine işaret etmektedir." [1, 2, 3]

Anahtar Kelimeler: 2-Etoksi-5-floro-1H-pirimidin-4-on,Atomik yük dağılımı,UV-Vis spektroskopisi

Abstract

A comprehensive quantum-chemical investigation of 2-ethoxy-5-fluoro-1H-pyrimidin-4-one ($C_6H_7FN_2O_2$) was carried out using density functional theory (DFT) and Hartree–Fock (HF) methods at the B3LYP/6-31+G(d,p) and HF/6-31+G(d) levels to elucidate its structural, spectroscopic, thermochemical, charge distribution, and electronic properties. The optimized geometry reveals a stable heterocyclic structure in which the pyrimidinone ring, fluorine substituent, carbonyl group, and ethoxy moiety collectively govern the molecular electronic structure. The calculated geometrical parameters indicate good agreement between the theoretical approaches, confirming the reliability of the optimized molecular model. Theoretical 1H and 13C NMR chemical shifts were evaluated using the GIAO method and compared with available experimental data recorded in CDCl3. The DFT calculations reproduce the experimental chemical shifts more accurately than the HF method, highlighting the importance of electron-correlation effects in predicting magnetic shielding constants. Significant deshielding is observed for carbon atoms bonded to electronegative nitrogen, oxygen, and fluorine atoms, whereas the ethoxy-group carbons and hydrogen atoms exhibit comparatively lower chemical shifts. Atomic charge distributions were also analyzed using both Mulliken population and atomic polar tensor (APT) schemes. The results reveal pronounced electronic polarization within the molecule, with the carbonyl oxygen, fluorine atom, and pyrimidine nitrogen

n atoms carrying substantial negative charge densities, while several carbon and hydrogen atoms exhibit positive charge accumulation. The calculated charge distribution confirms the existence of efficient intramolecular charge redistribution regulated by the combined electron-withdrawing effects of fluorine and carbonyl functionalities. Additionally, thermochemical calculations indicate that the molecule possesses favorable energetic stability, while the calculated dipole moment displays its polar molecular nature. Frontier molecular orbital (FMO) analysis displays that the HOMO is mainly localized over the pyrimidinone ring and heteroatom-rich regions, whereas the LUMO is concentrated around the carbonyl- and fluorine-containing portions of the heterocyclic structure. This spatial separation facilitates intramolecular charge-transfer processes. The HOMO-LUMO energy gap together with the derived global reactivity descriptors, including electronegativity, chemical hardness, softness, chemical potential, and electrophilicity index, indicate a balanced combination of electronic stability and chemical reactivity. UV-Vis spectral analysis reveals that the electronic absorption behavior is dominated by $\pi \rightarrow \pi^*$ and $n \rightarrow \pi^*$ transitions involving the conjugated heterocyclic system and heteroatom lone-pair electrons. Furthermore, electrostatic potential (ESP) and molecular electrostatic potential (MEP) analyses identify the carbonyl oxygen atom, fluorine atom, and ring nitrogen atoms as the most electron-rich regions, while the N-H and ethoxy hydrogen atoms constitute the principal positive potential zones. All in all, the theoretical results obtained show that 2-ethoxy-5-fluoro-1H-pyrimidin-4-one possesses a highly polarized electronic structure, well-defined reactive centers, and favorable charge-transfer characteristics. The findings provide a detailed understanding of its structural stability, spectroscopic behavior, and reactivity patterns, suggesting potential relevance in pharmaceutical, agrochemical, and functional-material applications.

Keywords: 2-Ethoxy-5-fluoro-1H-pyrimidin-4-one, Atomic charge distribution, UV-Vis spectroscopy.

1. Introduction

Heterocyclic compounds containing pyrimidine rings constitute one of the most important classes of organic molecules owing to their central role in medicinal chemistry, biochemistry, and materials science. Pyrimidine derivatives form the structural backbone of several naturally occurring nucleobases and exhibit a broad spectrum of biological activities, including antiviral, antibacterial, antifungal, antitumor, and anti-inflammatory properties. Consequently, understanding the structural and electronic characteristics of pyrimidine-based molecules has attracted considerable interest from both experimental and theoretical researchers (Brown et al,2000;Joule & Mills,2012; Katritzky et al.,2010).

Among fluorinated heterocycles, fluoropyrimidine derivatives have received particular attention because the introduction of fluorine significantly modifies molecular polarity, electronic distribution, metabolic stability, intermolecular interactions, and biological activity. Owing to its high electronegativity and small atomic radius, fluorine can alter charge density distribution and molecular reactivity without substantially perturbing the molecular structure. The characteristics mentioned have made fluorinated pyrimidines important building blocks in pharmaceutical synthesis and medicinal chemistry, especially in the development of antimetabolites, antiviral agents, and anticancer drugs (Hsu et al.,2026; Meanwell, 2018; Purser et al.,2008).

The compound investigated in the present work, 2-ethoxy-5-fluoro-4-pyrimidinone (also known as 2-ethoxy-5-fluoro-1H-pyrimidin-4-one, 2-ethoxy-5-fluoropyrimidin-4(1H)-one, 4(1H)-pyrimidin one, 2-ethoxy-5-fluoro-, and 5-fluoro-2-ethoxy-4-pyrimidinone), belongs to the fluorinated pyrimi dinone family and possesses the molecular formula $C_6H_7FN_2O_6$. The molecule contains a conjugated pyrimidinone ring incorporating two nitrogen atoms, a fluorine substituent, and an ethoxy functional group, providing a chemically versatile framework with potentially interesting electronic and spectroscopic properties (Hughes & O'Hagan, 2010; Noser et al., 2026; Sivaraman et al., 2026). Furthermore, this compound has been reported as an intermediate and impurity related to fluoropyrimidine-based pharmaceutical compounds and fluorouracil derivatives, further increasing its chemical significance.

From a molecular physics perspective, the coexistence of electron-withdrawing fluorine, heteroatomic nitrogen centers, and oxygen-containing functional groups generates a complex electronic environment regulated by intramolecular charge transfer, orbital delocalization, hydrogen-bonding tendencies, and tautomeric effects. The features discussed can strongly influence molecular stability, frontier molecular orbitals, dipole moment, nonlinear optical behavior, and spectroscopic signatures (Kawamura & Sanemitsu, 1993; Muthuraman et al., 2000; Nangia, 2006; Sharma et.,2002). Despite the potential importance of the fluorinated pyrimidinone derivative, detailed investigations concerning its electronic structure, quantum-chemical descriptors, charge-transfer characteristics, and spectroscopic properties remain relatively limited.

Recent advances in quantum computational theories such as Hartree-Fock (HF) and especially density functional theory (DFT) have provided powerful tools for investigating molecular systems at the atomic level. Particularly, DFT calculations enable accurate prediction of optimized molecular geometries, vibrational frequencies, electronic transitions, molecular electrostatic potential distributions, frontier molecular orbital energies, global reactivity descriptors, and intermolecular interaction sites. The integration

of experimental spectroscopy with quantum-chemical calculations therefore provides a comprehensive understanding of the structure-property relationships governing molecular behavior (Bayrakdar et al.,2026; Becke,1993; Dennington II et al.,2007; Frisch et al.,2009). Accordingly, the primary objective of the present study is to perform a comprehensive atomic and molecular-level investigation of 2-ethoxy-5-fluoro-4-pyrimidinone using advanced quantum-chemical approaches. Detailed analyses of molecular geometry, electronic structure, frontier molecular orbitals, charge distribution, molecular electrostatic potential, global reactivity descriptors, and spectroscopic characteristics are conducted to elucidate the fundamental physicochemical properties of this fluorinated pyrimidinone derivative. The obtained results are expected to contribute to a deeper understanding of fluorinated heterocyclic compounds and to provide valuable theoretical insight for future pharmaceutical, chemical, and materials-related applications.

The presence of a fluorine substituent, an ethoxy functional group, and a heteroaromatic pyrimidinone ring makes 2-ethoxy-5-fluoro-4-pyrimidinone ($C_6H_7FN_2O_2$) an attractive molecular system for both experimental and theoretical investigations. The coexistence of electron-withdrawing fluorine atoms and electron-donating alkoxy groups within the same conjugated heterocyclic framework generates a complex electronic environment characterized by charge redistribution, orbital delocalization, and intramolecular polarization effects. Furthermore, pyrimidinone derivatives constitute an important class of heterocyclic compounds widely employed as intermediates in pharmaceutical synthesis, medicinal chemistry, and biologically active molecular architectures. Consequently, understanding the relationship between molecular structure, electronic configuration, and chemical reactivity is essential for elucidating the physicochemical behavior of such fluorinated heterocyclic systems (Lee et al., 1998; Stephens et al., 1994).

In recent decades, computational quantum chemistry has emerged as an indispensable tool for investigating molecular systems at the atomic and electronic levels. The rapid development of computational methodologies and high-performance computing resources has enabled the accurate prediction of structural, spectroscopic, thermodynamic, and electronic properties that are often difficult or impossible to determine exclusively through experimental techniques (Antony& Grimme,2006; Francl et al.,1982). Among the available theoretical approaches, HF and DFT calculation methods remain the most widely utilized methods for studying organic and heterocyclic molecules owing to their favorable balance between computational efficiency and predictive accuracy (Tsuzuki & Uchimaru, 2020).

The HF method represents one of the earliest and most fundamental ab initio quantum-mechanical approaches for solving the many-electron Schrödinger equation. Within the self-consistent field (SCF) framework, each electron is assumed to move in the average electrostatic field generated by all other electrons. The molecular wavefunction is expressed as a single Slater determinant, ensuring compliance with the Pauli exclusion principle and antisymmetry requirements. Although HF accurately accounts for exchange interactions, it neglects dynamic electron-correlation effects arising from instantaneous electron–electron interactions. As a consequence, HF calculations often overestimate total energies, HOMO-LUMO energy gaps, and molecular stability while underestimating electron delocalization phenomena (Young, 2001). Nevertheless, HF calculations provide valuable baseline information regarding molecular geometries, orbital

distributions, atomic charge populations, and electronic structure trends, making them useful reference points for more sophisticated theoretical methods.

To overcome the limitations associated with the neglect of electron correlation, DFT calculations has become the dominant computational framework in modern molecular physics and computational chemistry. Unlike wavefunction-based approaches, DFT describes the electronic system through the electron density as the fundamental variable, substantially reducing computational complexity while maintaining high accuracy. The theoretical foundations established by Hohenberg, Kohn, and Sham demonstrated that the ground-state properties of many-electron systems can be uniquely determined from the electron density distribution (Laury et al., 2012; Parr, 1989). In particular, hybrid exchange-correlation functions such as B3LYP, which combine exact HF exchange with gradient-corrected correlation functions, have proven highly successful for predicting molecular structures, vibrational frequencies, dipole moments, charge-transfer characteristics, and electronic properties of organic molecules (Koopmans, 1934). On this basis, compared with HF calculations, DFT level of theory provides a more realistic description of electron correlation effects, accordingly improving the prediction of bond lengths, bond angles, total energies, ionization potentials, electron affinities, and frontier molecular orbital energies. Furthermore, DFT enables detailed analyses of molecular electrostatic potential (MEP) surfaces, natural bond orbital (NBO) interactions, charge-transfer pathways, chemical hardness, electrophilicity, nucleophilicity, and other global reactivity descriptors. These parameters play a critical role in understanding intermolecular interactions, biological activity, spectroscopic behavior, and the fundamental chemical reactivity of heterocyclic compounds (Gokce et al.,2024).

The combined application of HF and DFT methodologies displays a comprehensive theoretical framework for investigating the electronic behavior of 2-ethoxy-5-fluoro-4-pyrimidinone. Comparative analyses between the two methods allow assessment of the role of electron correlation in determining molecular stability, geometric parameters, and electronic distributions. Moreover, detailed examination of frontier molecular orbitals (HOMO and LUMO), energy-gap characteristics, molecular electrostatic potential maps, and global reactivity descriptors provides valuable insight into charge-transfer mechanisms, reactive sites, intermolecular interactions, and potential physicochemical applications of the molecule.

Accordingly, the primary objective of the present study is to perform a comprehensive quantum-chemical investigation of 2-ethoxy-5-fluoro-4-pyrimidinone using HF and DFT approaches. Optimized molecular geometries, total energies, electronic structures, charge distributions, spectroscopic findings, frontier molecular orbitals, molecular electrostatic potential distributions, and reactivity parameters are systematically analyzed to establish fundamental structure–property relationships. The results obtained are expected to contribute to a deeper understanding of fluorinated pyrimidinone derivatives and provide theoretical guidance for future studies involving heterocyclic pharmaceuticals, molecular electronics, and functional organic materials.

2. Computational Details for 2-Ethoxy-5-Fluoro-4-Pyrimidinone

A comprehensive quantum-chemical investigation was performed to elucidate the structural, electronic, thermodynamic, atomic charge distributions (Mulliken population analysis and the Atomic Polar Tensor),

nuclear magnetic resonance (^{1}H and ^{13}C) chemical shifts, and fundamental optical properties of 2-ethoxy-5-fluoro-4-pyrimidinone with the formula of $C_6H_7FN_2O_2$. The title molecule belongs to the fluorinated pyrimidinone family, featuring a central heteroaromatic pyrimidine ring. It is characterized by a fluorine atom attached to the fifth carbon (C_5) and an ethoxy group at the second carbon (C_2). The chemical impact of these specific substitutions depends heavily on the molecular structure of title molecule. The simultaneous presence of electron-withdrawing fluorine and electron-donating ethoxy functionalities within the same conjugated heterocyclic framework generates a complex electronic environment characterized by charge redistribution, orbital hybridization, and intramolecular polarization effects. Furthermore, the carbonyl oxygen and ring nitrogen atoms introduce additional possibilities for electron delocalization, resonance stabilization, and intermolecular interactions. The mentioned structural features make 2-ethoxy-5-fluoro-4-pyrimidinone an attractive molecular system for detailed theoretical investigation.

Full geometry optimization calculations were initially carried out to determine the equilibrium structure corresponding to the global minimum on the potential energy surface so as to obtain a fundamental understanding of the physicochemical behavior of the title compound. Subsequently, a series of quantum-chemical analyses, including thermodynamic parameter calculations, frontier molecular orbital (HOMO-LUMO) analysis, molecular electrostatic potential (MEP) mapping, electrostatic potential (ESP) surface visualization, total electron-density distribution, and simulated UV–Vis absorption spectra, were performed for 2-ethoxy-5-fluoro-4-pyrimidinone for the first time. These calculations provide detailed information about molecular stability, charge-transfer behavior, electron delocalization pathways, and the influence of fluorine and ethoxy substituents on the electronic structure of the pyrimidinone framework. Moreover, the MEP and ESP surfaces facilitate the identification of electrophilic and nucleophilic regions, allowing prediction of potential reactive sites and intermolecular interaction centers within the molecule. The obtained scientific results enable us to better understand the molecular reactivity, electronic structure, intramolecular charge transfer (ICT), and aromatic electron delocalization, with particular emphasis on the influence of the electron-withdrawing substituents.

All quantum-chemical calculations were carried out within the framework of Density Functional Theory (DFT) using the widely employed B3LYP hybrid exchange–correlation functional (Laury et al.,2012; Tsuzuki & Uchimaru, 2020; Young, 2001). The B3LYP functional combines Becke's three-parameter exchange functional with the Lee-Yang-Parr correlation functional and has demonstrated excellent reliability in predicting the structural, energetic, and electronic properties of heterocyclic organic molecules. The 6-31G(d,p) basis set (Parr, 1989), which includes polarization functions on all atoms, was employed to achieve an accurate description of molecular geometry, charge redistribution, and orbital interactions. The inclusion of polarization functions is particularly important for properly describing the lone-pair electrons associated with the nitrogen and oxygen atoms as well as the strong electronegativity effects introduced by fluorine substitution.

To further evaluate the electronic behavior and chemical reactivity of the title compound, several global quantum-chemical descriptors were calculated from the frontier molecular orbital energies according to Koopmans' approximation. These descriptors include the ionization potential (I), electron affinity (A), chemical softness (S), chemical hardness (η), electronegativity (χ), chemical potential (μ), electrophilicity

index (ω), maximum electronic charge-transfer capability (ΔN_{max}), and also HOMO–LUMO energy gap (ΔE) parameters. Such parameters provide quantitative information regarding molecular stability, kinetic reactivity, electron-donating and electron-accepting tendencies, and the charge-transfer characteristics of 2-ethoxy-5-fluoro-4-pyrimidinone.

In addition, time-dependent density functional theory (TD-DFT) calculations and ZINDO computation methods were performed in the gas phase to simulate the electronic absorption spectrum and investigate the nature of electronic transitions responsible for the optical response of the molecule. The calculated excited-state properties were used to identify the dominant orbital contributions involved in the absorption process and to evaluate possible ICT transitions between the heteroaromatic pyrimidine ring and the substituent groups.

All quantum-chemical computations were performed using the Gaussian 09 software package (Koopmans,1934). Molecular visualization, frontier molecular orbital plotting, electron-density analysis, electrostatic potential mapping, and graphical representations were generated using GaussView and related molecular visualization tools (Gökce et al., 2024). The obtained theoretical results provide a detailed atomic-scale description of the structural, electronic, optical, and reactive properties of 2-ethoxy-5-fluoro-4-pyrimidinone and establish a foundation for understanding its physicochemical behavior and potential applications in heterocyclic and pharmaceutical chemistry.

3. Results and Discussion

3.1 Optimized Molecular Geometry of 2-Ethoxy-5-Fluoro-1H-pyrimidin-4-one

A detailed understanding of the molecular geometry of 2-ethoxy-5-fluoro-1H-pyrimidin-4-one is essential for elucidating its electronic structure, intermolecular interactions, and physicochemical behavior. The molecule consists of a fluorinated pyrimidinone ring bearing an ethoxy substituent, where the combined effects of heteroatoms, conjugation, and substituent-induced electronic polarization significantly influence the structural characteristics of the system (Noser et al., 2026; Sivaraman et al., 2026). To obtain reliable geometrical parameters, full geometry optimizations were performed using both DFT/B3LYP/6-31+G(d,p) and HF/6-31+G(d,p) computational approaches. The optimized structure corresponding to the minimum-energy configuration was identified as the most stable conformer and subsequently employed for all theoretical investigations. The optimized molecular geometry together with the atom-numbering scheme is presented in Fig. 1.

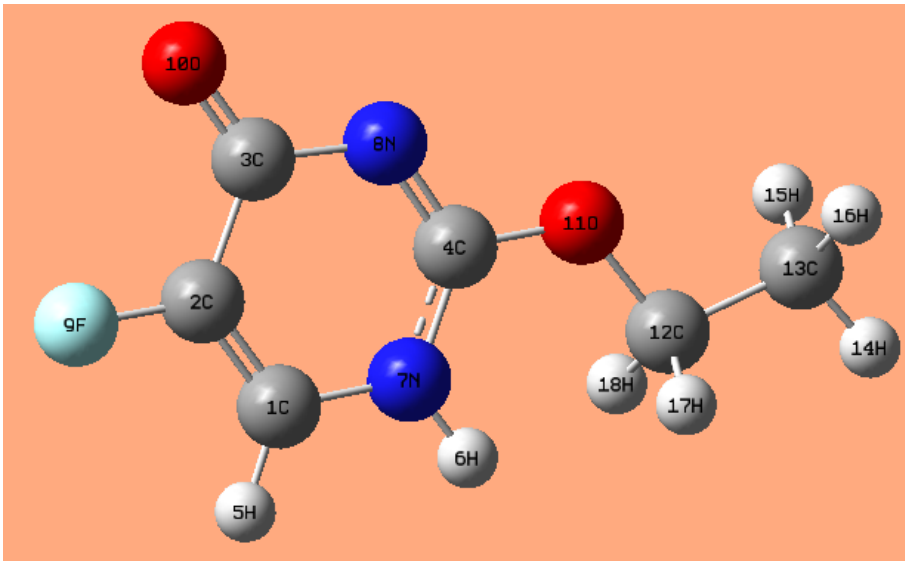

Figure 1. Optimized molecular structure pertaining to 2-ethoxy-5-fluoro-1H-pyrimidin-4-one

Selected bond lengths and bond angles calculated at the DFT/B3LYP/6-31+G(d,p) and HF/6-31+G(d,p) levels are summarized in Tables 1 and 2 in detail. To assess the consistency of the computational approaches, correlation analyses were carried out for the calculated geometrical parameters. The corresponding correlation plots are shown in Figs. 2 and 3. Excellent agreement between the two theoretical methods was obtained for bond length sizes, indicating that both approaches provide a reliable description of the molecular framework. The correlation coefficients are determined to be about 0.99678 for bond length distances and 0.90725 for bond angle parameters. Minor differences (especially for bond angles) observed between the HF and DFT results mainly originate from the treatment of electron-correlation effects.

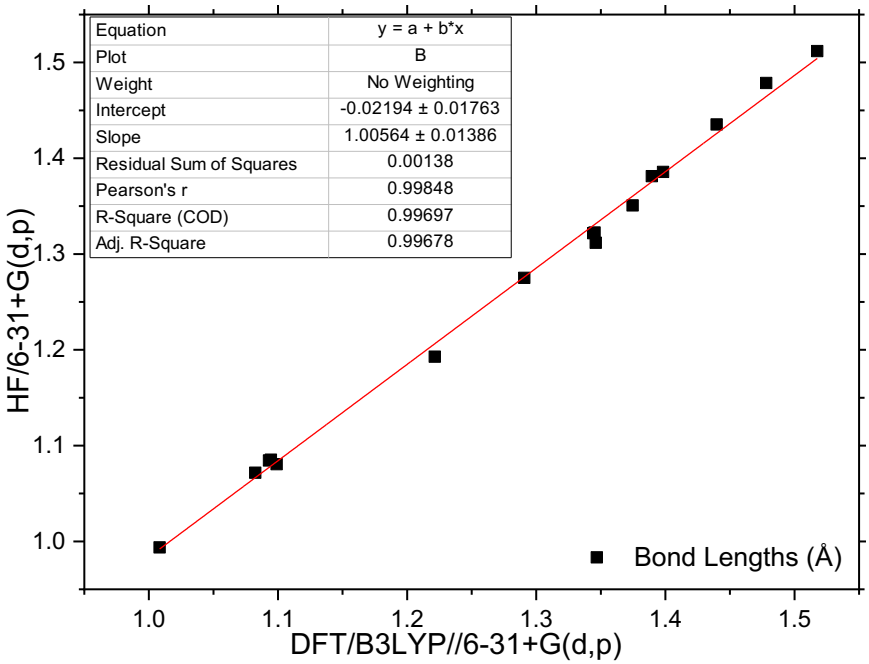

Figure 2. Bond length size correlations between HF and B3LYP calculation levels for 2-ethoxy-5-fluoro-1H-pyrimidin-4-one compound

The maximum difference between bond length sizes is noted as 0.0344 Å for the C4-O11 atoms, as provided in Table 1. Similarly, the largest variation is detected as 6.1584° for the N7-C4-O11 atoms, as provided in Table 2. It is apparent that the environment plays a serious role on the molecular geometry of 2-Ethoxy-5-fluoro-1H-pyrimidin-4-one compound. As expected, the HF method generally predicts slightly shorter bond distances and somewhat larger bond angles because electron correlation is not explicitly included in the HF calculation formalism. In contrast, the B3LYP functional accounts for electron correlation through the exchange-correlation potential, providing a more realistic representation of electron-density distribution within the molecule (Boo et al., 2007; Buyukuslu et al., 2010; Gökce & Bahçeli, 2025; Gökce, Bahçeli &Alpaslan, 2024; Jumabaev et al.,2024; Parlak et al.,2011; Sobczyk et al., 2005).Consequently, DFT calculation results better describe the effects of π-electron delocalization, lone-pair interactions, resonance stabilization, and intramolecular charge transfer occurring within the pyrimidinone ring.

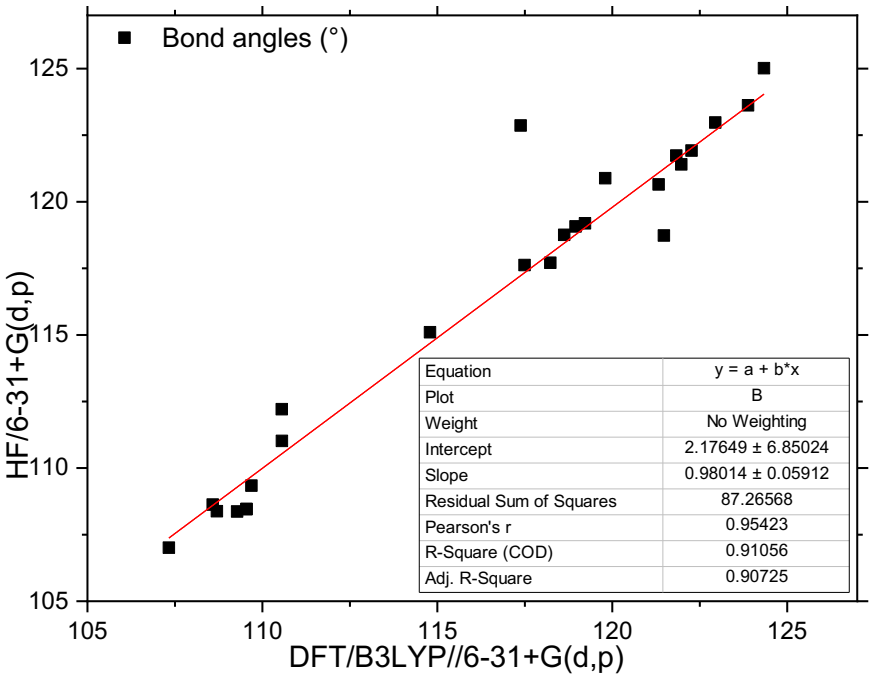

Figure 3. Bond angle correlations between HF and B3LYP calculation levels for 2-ethoxy-5-fluoro-1H-pyrimidin-4-one compound

In more detail, the optimized structure reveals that the pyrimidinone ring maintains an essentially planar geometry, which facilitates efficient electron delocalization throughout the heterocyclic framework. Hence, the C-O and C-C bonds associated with the ethoxy substituent exhibit values characteristic of alkoxy-functionalized heterocyclic systems. The ethoxy group adopts a conformation that minimizes steric repulsion while preserving favorable electronic communication with the pyrimidinone ring. Numerically, the C_3=O_{10} bond (1.2214 Å at DFT and 1.1929 Å at HF) of the pyrimidinone moiety exhibits the characteristic features of a carbonyl double bond, whereas the bond length distances of C_4-O_{11} and C_{12}-O_{11} bonds are calculated to be about 1.3461 Å and 1.4397 at B3LYP and 1.3117 Å and 1.4352 at HF calculation methods, respectively. As expected, the single bond length is longer than the double bond between the oxygen and carbon atoms. Moreover, the adjacent C-N and C-C bonds show intermediate bond lengths arising from resonance effects within the conjugated system. In this respect, the bond distances between C_1-N_7 and C_4-N_7 atoms are

computed as 1.3896 Å and 1.3747 Å at DFT/B3LYP//6-31+G(d,p) and 1.3813 Å and 1.3507 Å at HF/6-31+G(d,p) calculation levels, respectively. Besides, the length between H_6 and N_7 atoms is found to be about 1.0083 Å and 0.9937 Å using DFT and HF calculation levels of theory, respectively. the difference stems from the conjugated atom effect and delocalization. As for the bond length sizes between carbon and carbon atoms, the highest calculation is obtained as 1.5176 Å and 1.5118 Å for C12-C13 length, whereas the minimum lengths of 1.3452 Å and 1.3225 Å ascribes to bond length for C1-C2 atoms at DFT/B3LYP//6-31+G(d,p) and HF/6-31+G(d,p) levels of theory, respectively.

Table 1. Theoretical bond length sizes for optimized geometric parameters of 2-ethoxy-5-fluoro-1H-pyrimidin-4-one molecule

	Bond lengths (Å)	
Atoms	**DFT/B3LYP/6-31G(d,p)**	**HF/6-31G(d,p)**
C_1-C_2	1.3452	1.3225
C_1-H_5	1.0824	1.0717
C_1-N_7	1.3896	1.3813
C_2-C_3	1.4781	1.4786
C_2-F_9	1.3441	1.3217
C_3-N_8	1.3982	1.3857
C_3-O_{10}	1.2214	1.1929
C_4-N_7	1.3747	1.3507
C_4-N_8	1.2908	1.2751
C_4-O_{11}	1.3461	1.3117
H_6-N_7	1.0083	0.9937
O_{11}-C_{12}	1.4397	1.4352
C_{12}-C_{13}	1.5176	1.5118
C_{12}-H_{17}	1.099	1.0806
C_{12}-H_{18}	1.099	1.0806
C_{13}-H_{14}	1.0945	1.0853
C_{13}-H_{15}	1.0931	1.0844
C_{13}-H_{16}	1.0931	1.0844

At the same time, the presence of electronegative nitrogen and fluorine atoms induces noticeable polarization of neighboring bonds, leading to slight deviations from idealized bond parameters. In this context, the bond lengths between carbon and nitrogenous atoms are determined to be about 1.3982 Å and 1.2908 Å at DFT method and 1.3857 Å and 1.2751 Å at HF calculation level of theory, respectively. The C-F bond length falls within the typical range reported for fluorinated heteroaromatic compounds, revealing the strong electronegativity and electron-withdrawing nature of fluorine. On this basis, the length of C_2-F_9 atoms is computed as about 1.3441 (DFT) and 1.3217 (HF). Additionally, the bond lengths between carbon and hydrogen atoms are determined between 1.0990 Å (C_{12}-H_{17} and C_{12}-H_{18}) and 1.0824 Å (C_1-H_5) at DFT/B3LYP//6-31+G(d,p) and 1.0853 Å (C13-H14) and 1.0717 Å (C1-H5) at HF/6-31+G(d,p) levels of theory, respectively.

Table 2. Theoretical bond angles for optimized geometric parameters of 2-ethoxy-5-fluoro-1H-pyrimidin-4-one molecule

	Bond angles (°)	
Atoms	**DFT**	**HF**
C_2-C_1-H_5	123.8802	123.6194
C_2-C_1-N_7	118.6273	118.7556
H_6-C_1-N_7	117.4925	117.625
C_1-C_2-C_3	121.9714	121.4048
C_1-C_2-F_9	119.798	120.886
C_3-C_2-F_9	118.2306	117.7092
C_2-C_3-N_8	114.79	115.1003
C_2-C_3-O_{10}	122.2662	121.923
N_8-C_3-O_{10}	122.9438	122.9767
N_7-C_4-N_8	124.3378	125.0154
N_7-C_4-O_{11}	118.2785	112.1201
N_8-C_4-O_{11}	117.3836	122.8646
C_1-N_7-C_4	118.9495	119.0734
C_1-N_7-H_4	119.221	119.1921
C_4-N_7-H_6	121.8295	121.7344
C_3-N_8-C_4	121.324	120.6505
C_4-O_{11}-C_{12}	121.4767	118.7302
O_{11}-C_{12}-C_{13}	107.3287	107.0097
O_{11}-C_{12}-H_{17}	109.5467	108.4578
O_{11}-C_{12}-H_{18}	109.5473	108.4578
C_{13}-C_{12}-H_{17}	110.5559	112.2091
C_{13}-C_{12}-H_{18}	110.5559	112.209
H_{17}-C_{12}-H_{18}	109.2778	108.3687
C_{12}-C_{13}-H_{14}	109.6885	109.3423
C_{12}-C_{13}-H_{15}	110.5603	111.0192
C_{12}-C_{13}-H_{16}	110.5587	111.0192
H_{14}-C_{13}-H_{15}	108.7014	108.3768
H_{14}-C_{13}-H_{16}	108.7015	108.3768
H_{15}-C_{13}-H_{16}	108.5811	108.6291

The calculated bond angles within the heterocyclic ring are generally close to the values expected for an sp^2-hybridized conjugated system. Small deviations from ideal trigonal-planar geometry arise from the presence of heteroatoms, the carbonyl functionality, and substituent-induced electronic effects. The nearly planar arrangement of the ring atoms promotes conjugation and contributes to the stability of the 2-ethoxy-5-fluoro-1H-pyrimidin-4-one molecular structure.

All in all, the optimized geometry demonstrates that 2-ethoxy-5-fluoro-1H-pyrimidin-4-one possesses a rigid and highly conjugated heterocyclic framework with significant electron delocalization. The structural parameters obtained from both HF and DFT quantum calculations exhibit good agreement and confirm the suitability of the selected computational methodology for describing the molecular architecture of the title compound. The geometrical results obtained provide a reliable basis for subsequent analyses of electronic properties, charge distribution, spectroscopic behavior, and intermolecular interactions.

3.2 Thermochemical Properties of 2-Ethoxy-5-Fluoro-1H-pyrimidin-4-one Molecular Structure

The thermochemical properties of 2-ethoxy-5-fluoro-1H-pyrimidin-4-one were investigated using the DFT/B3LYP and HF methods with the 6-31+G(d,p) basis set to evaluate its energetic stability, thermal behavior, and molecular polarity. Thermodynamic parameters obtained from the optimized molecular geometry, including total electronic energy, zero-point vibrational energy (ZPVE), thermal energy, entropy, heat capacity, rotational constants, and dipole moment components, are summarized in Table 3. The zero-point vibrational energies were corrected using appropriate scaling factors of 0.977 for B3LYP and 0.909 for HF method to compensate for the systematic overestimation of harmonic vibrational frequencies. The absence of imaginary frequencies in the optimized structure confirms that the molecule resides at a true minimum on the potential energy surface, indicating the stability of the optimized configuration. The calculated total electronic energies display the stabilization arising from conjugation within the pyrimidinone ring and the electronic effects of the fluorine, carbonyl, nitrogen, and ethoxy substituents. According to table, total electronic energy values for 2-ethoxy-5-fluoro-1H-pyrimidin-4-one molecule are found to be about -592.65749664 and -589.37101891 a.u. at B3LYP/6-31+G(d,p) and HF/6-31G+(d,p) levels of theory. The ZPVE values provide valuable information regarding the intrinsic vibrational stability of the molecule. The vibrational contributions arise primarily from C=O stretching, C-F vibrations, N-H motions, C-N and C-O bond vibrations, as well as skeletal deformations of the heterocyclic ring. The presence of multiple heteroatoms significantly influences the vibrational energy distribution and contributes to the overall thermodynamic stability of the system (Mohammadi et al., 2023; Xiao et al., 2017). Accordingly, the scaled ZPVE parameters are determined as about 81.88557456 and 82.58282271 kcal.mol^{-1} at DFT/B3LYP//6-31G(d,p) and HF/6-31G(d,p) calculation levels, respectively. The models point out the zero-point correction values of about 0.133565 and 0.144779 kcal.mol^{-1}, respectively. Furthermore, these values verify the energetic stability of the molecular framework and indicate an extended network of partial π-electron delocalization encompassing the aromatic, carbonyl, and alkoxy-functionalized heterocyclic systems.

The entropy values are derived from translational, rotational, and vibrational contributions, with the vibrational component representing a substantial fraction of the total entropy due to the large number of accessible vibrational modes associated with the heterocyclic framework and the ethoxy substituent. On this basis, the total entropy is calculated to be 101.078 and 97.190 cal mol^{-1} K^{-1}, comprising translational (41.082 and 41.082), rotational (30.311 and 30.244), and vibrational (29.684 and 25.863) contributions.

Table 3. Fundamental thermodynamic quantities: heat capacities (cal mol^{-1} K^{-1}), entropies (cal mol^{-1} K^{-1}), thermal energies (cal mol^{-1} K^{-1}), zero-point energies (kcal mol^{-1}), zero-point corrections (Hartree/Particle), dipole moment (Debye), and rotational constants (GHz) for 2-ethoxy-5-fluoro-1H-pyrimidin-4-one molecule.

Parameters	**DFT/B3LYP//6-31+(d,p)**	**HF/6-31+(d,p)**
Total energy	-592.65749664	-589.37101891
Zero-point vibrational energy	81.88557456	82.58282271
Zero-point correction	0.133565	0.144779
Thermal correction to Energy	0.143923	0.154339
Thermal correction to Enthalpy	0.144867	0.155283
Thermal correction to Gibbs Free Energy	0.096842	0.109105
Sum of electronic and zero-point Energies	-592.523932	-589.226240
Sum of electronic and thermal Energies	-592.513574	-589.216680
Sum of electronic and thermal Enthalpies	-592.512630	-589.215736
Sum of electronic and thermal Free Energies	-592.560655	-589.261914
Rotational constant	3.00642	2.87807
	0.58011	0.61900
	0.48930	0.51265
Entropy		
Total	101.078	97.190
Translational	41.082	41.082
Rotational	30.311	30.244
Vibrational	29.684	25.863
Heat capacity		
Total	37.321	34.481
Translational	2.981	2.981
Rotational	2.981	2.981
Vibrational	31.360	28.520
Thermal Energy		
Total	90.313	96.849
Translational	0.889	0.889
Rotational	0.889	0.889
Vibrational	88.535	95.072
μ_x	7.1762	-4.8287
μ_y	-7.5607	-6.3334
μ_z	0.0004	0
μ	10.4241	7.9642

Likewise, the calculated heat capacities indicate the ability of the molecule to absorb and store thermal energy through vibrational excitation processes. The relatively large vibrational contribution demonstrates that internal molecular motions play a dominant role in determining the thermal behavior of the compound. Hence, the molar heat capacity at constant volume (C_v) displays the thermal energy stored primarily via the vibrational excitations of the functional groups and the aromatic ring. As detailed in Table 3, the DFT/B3LYP model calculation yields a total C_v of 37.321 cal mol^{-1} K^{-1} (comprising 2.981 translational,

2.981 rotational, and 31.360 vibrational contributions). In comparison, the HF computational method results in a total C_v of 34.481 cal mol^{-1} K^{-1} (with 2.981 translational, 2.981 rotational, and 28.520 vibrational parts). Similarly, the total thermal energies are determined as about 90.313 cal mol^{-1} K^{-1} (with 0.889 translational, 0.889 rotational, and 88.535 vibrational parts) and 96.849 cal mol^{-1} K^{-1} (with 0.889 translational, 0.889 rotational, and 95.072 vibrational parts) at DFT and HF calculation techniques, respectively. The calculated rotational constants (A, B, and C) confirm that 2-ethoxy-5-fluoro-1H-pyrimidin-4-one behaves as an asymmetric-top molecule. This behavior originates from the non-uniform mass distribution generated by the fluorine atom, carbonyl group, ring nitrogen atoms, and ethoxy side chain. Although the pyrimidinone ring remains essentially planar, the ethoxy substituent introduces a degree of conformational flexibility that contributes to the asymmetric rotational characteristics. Calculated at the DFT/B3LYP//6-31G(d,p) and HF/6-31+G(d,p) levels of theory, respectively, the rotational constants are 3.00642 (2.87807) GHz, 0.58011 (0.61900) GHz, and 0.48930 (0.51265) GHz, indicating an asymmetric top molecular configuration. The dipole moment constitutes an important descriptor of molecular behavior. For the title compound, the total dipole moments are calculated to be 10.4241 D (B3LYP) and 7.9642 D (HF). The corresponding Cartesian components (μ_x, μ_y, and μ_z) are 7.1762, -7.5607, and 0.0004 D for the B3LYP model, compared to -4.8287, -6.3334, and 0 D for the HF model. The calculated dipole moment components indicate a significant degree of molecular polarity arising from the combined electron-withdrawing effects of the fluorine atom and carbonyl group together with the electron-donating character of the ethoxy substituent. Furthermore, the presence of ring nitrogen atoms enhances charge separation within the molecular framework. Such electronic polarization facilitates intermolecular interactions, including dipole-dipole attractions, hydrogen bonding, and charge-transfer processes, which may be important for the biological and physicochemical properties of the compound (Fanchini et al., 2002; Synder & Carlsen, 1977; Xu et al., 2024; Zhou & Umezawa, 2015).

To sum up, the thermochemical results demonstrate that 2-ethoxy-5-fluoro-1H-pyrimidin-4-one is an energetically stable and polar heterocyclic system. Its thermodynamic behavior is governed by the synergistic effects of heteroatom substitution, π-electron delocalization, and intramolecular charge redistribution, providing a solid foundation for understanding its electronic structure and spectroscopic properties.

3.3 UV–Vis Spectral Analysis

The electronic absorption properties of 2-ethoxy-5-fluoro-1H-pyrimidin-4-one were investigated to gain insight into its excited-state behavior and optical characteristics. The UV–Vis spectrum was simulated using time-dependent density functional theory (TD-DFT), time-dependent Hartree-Fock, and ZINDO calculation methods, and the major electronic transitions were analyzed in terms of excitation energies, oscillator strengths, and frontier orbital contributions. Since the results were close to each other, the calculated transitions determined by ZINDO calculation model (Steinmann et al., 2011) are summarized in Table 4.

The absorption behavior of the molecule is primarily governed by the conjugated pyrimidinone ring, the carbonyl group, the fluorine substituent, and the ethoxy functionality. Owing to the presence of heteroatoms with non-bonding electron pairs and an extended π-electron framework, the observed electronic transitions mainly involve π→π* and n→π* excitations. These transitions are characteristic of heterocyclic carbonyl-containing systems and significantly influence the optical response of the molecule (Tortorella et al., 2016).

The most intense absorption bands originate predominantly from π→π* transitions involving the frontier molecular orbitals. The HOMO is mainly localized over the pyrimidinone ring, oxygen atoms, and nitrogen-containing regions, whereas the LUMO is distributed over the conjugated heterocyclic framework and carbonyl-containing portions of the molecule. This orbital arrangement facilitates intramolecular charge redistribution upon excitation and contributes to the electronic polarization of the system.

In addition to the dominant π→π* transitions, weaker n→π* transitions are observed due to excitation of lone-pair electrons located on the oxygen and nitrogen atoms. The mentioned transitions generally exhibit lower oscillator strengths because they are partially symmetry-forbidden; however, they remain important for understanding the photophysical behavior of the molecule.

Table 4. Theoretical absorption spectra (ZINDO) for 2-ethoxy-5-fluoro-1H-pyrimidin-4-one molecule.

Cl-expansion coefficient					
Excitations	**Energy (eV)**	**Singlet-A**	**Wavelength (nm)**	**Oscillator strength (f)**	**Translations**
Excited State 1					
41→43	2.8272	0.63886	438.54	0.00051	HOMO→LUMO+1
41→44		-0.11908			HOMO→LUMO+2
41→46		-0.27711			HOMO→LUMO+4
Excited State 2					
42→43	3.9973	0.30663	310.17	0.0446	LUMO→ LUMO+1
42→44		0.62133			LUMO→ LUMO+2
Excited State 3					
39→43 37→38	4.0348	0.27549	307.28	0.0030	HOMO-2→ LUMO+1
41→42		0.44289			HOMO→LUMO

The calculated absorption wavelengths and oscillator strengths indicate that the electronic transitions are strongly influenced by the electron-withdrawing fluorine atom and carbonyl group. The fluorine substituent modifies the electron density distribution within the pyrimidine ring, while the carbonyl group introduces low-lying antibonding orbitals that participate in electronic excitation processes. The ethoxy substituent further contributes to electron delocalization and affects the intensity of the absorption bands through inductive and resonance interactions.

The simulated spectrum displays that electronic excitation is accompanied by efficient charge redistribution within the heterocyclic framework. Such behavior is indicative of moderate intramolecular charge-transfer character, which is commonly observed in fluorinated heterocyclic compounds containing electron-rich and electron-deficient regions within the same molecular skeleton.

As shown in the table, the first excited state (λ_{max}=438.54 nm, meaning bang gap energy of 2.8272 eV) is mainly attributed to an n→π* transition. This weakly allowed transition (f=0.00051) originates from the interaction of lone-pair electrons on the heteroatoms with the aromatic π* orbitals. The second absorption band at 310.17 nm (3.9973 eV) corresponds to overlapping π→π* transitions enhanced by conjugation and electron delocalization within the aromatic framework, despite exhibiting an oscillator strength of 0.0446. In contrast, the intense band observed at 307.28 nm (f=0.0030) is assigned to a strongly allowed π→π*

transition involving aromatic bonds and interactions with substituent groups. Ultimately, the simulated absorption spectrum dispalys the combined influence of aromatic conjugation, substituent-induced electron withdrawal, and molecular asymmetry. Furthermore, the calculated excitation energies align with the HOMO-LUMO energy gap obtained from our DFT calculations, confirming the internal consistency of the theoretical results

In summary, the UV-Vis analysis reveals that the optical properties of 2-ethoxy-5-fluoro-1H-pyrimidin-4-one are governed by a combination of $\pi\rightarrow\pi^*$ and $n\rightarrow\pi^*$ electronic transitions involving the pyrimidinone ring, carbonyl group, fluorine atom, and ethoxy substituent. The observed charge-transfer characteristics and electronic delocalization reveal potential relevance of this molecule in pharmaceutical chemistry, molecular recognition studies, and functional organic materials exhibiting photoresponsive behavior.

3.2. Atomic Charge Distribution Analysis

Atomic charge distribution analysis is an effective approach for elucidating the electronic structure, polarization behavior, and potential reactive centers of molecular systems. In the present work, the charge distribution of 2-ethoxy-5-fluoro-1H-pyrimidin-4-one was investigated using both Mulliken population analysis and the APT quantum calculation method at the B3LYP/6-31+G(d,p) and HF/6-31+G(d,p) levels of theory. The calculated atomic charges are summarized in Table 5.

The Mulliken scheme provides information about electron partitioning among atoms based on molecular orbital populations, whereas the APT method evaluates atomic charges from the response of the molecular dipole moment to atomic displacements, thereby offering a more physically meaningful description of molecular polarization and vibrational charge transfer. Although the two approaches yield different absolute charge magnitudes, they display similar trends regarding electron-rich and electron-deficient regions within the molecule (Ibrahim et al., 2026).

For the carbon atoms, significant variations in charge distribution are observed depending on the local chemical environment. At the B3LYP/6-31+G(d,p) level, the APT charges range from +0.043928 (C_{13}) to +1.335555 (C_4), while the HF calculations produce values between +0.103341 (C_{13}) and +1.534791 (C_4). The largest positive charges are associated with the pyrimidinone ring carbons directly influenced by neighboring electronegative heteroatoms, indicating substantial electron withdrawal from these centers. Mulliken charges exhibit a wider distribution, varying from −0.608786 (C_{13}) to +0.585759 (C_4) at the DFT level and from −0.513265 (C_{13}) to +0.660533 (C_4) at the HF level. These results reveal pronounced electronic polarization within the heterocyclic ring and demonstrate the strong influence of adjacent nitrogen, oxygen, and fluorine atoms on the carbon charge distribution.

The heteroatoms exhibit the most distinctive charge characteristics. The two ring nitrogen atoms carry substantial negative charges in all computational models. At the DFT level, the Mulliken charges of N_7 and N_8 atoms are calculated to be about -0.396664 and -0.524394, respectively, while the corresponding APT charges are -0.660181 and -0.911363. Similar trends are obtained from HF calculations, where the Mulliken charges are -0.601210 (N_7) and -0.563892 (N_8) and the APT charges reach -0.844255 (N7) and -1.058551 (N_8). These pronounced negative values indicate significant electron accumulation around the nitrogen centers due to their high electronegativity and lone-pair electrons.

Likewise, the oxygen atoms associated with the carbonyl and ethoxy functionalities possess strongly negative charges. Within the DFT/APT calculations, O_{10} and O_{11} exhibit charges of -0.835030 and -0.977192, respectively, whereas the HF/APT computational method yields even more negative values of -0.995593 and -1.124224. Mulliken charges for these oxygen atoms vary between -0.274202 and -0.446017 at the DFT/6-31+G(d,p) level and between -0.521789 and -0.538003 at the HF/6-31+G(d,p) level of theory. The substantial negative charge concentration around oxygen atoms reflects strong localization of lone-pair electrons and highlights their importance as potential sites for electrophilic interactions and hydrogen-bond acceptance. The fluorine atom (F_9) also exhibits a marked negative charge due to its exceptionally high electronegativity. The calculated APT charge amounts to -0.526765 at the B3LYP level and -0.557283 at the HF level, while the Mulliken charges are determined as -0.355736 and -0.438026, respectively. The results calculated indicate considerable electron density localization around the fluorine atom, contributing to the overall molecular polarity and influencing intermolecular interactions.

Table 5 Point Atomic Charge Distributions of 2-ethoxy-5-fluoro-1H-pyrimidin-4-one molecule.

Label	**Atomic Charges (DFT/B3LYP/6-31+(d,p))**		**Atomic Charges (HF/6-31+(d,p))**	
	APT	**Mulliken**	**Mulliken**	**APT**
C_1	0.247416	-0.017684	0.192525	0.358597
C_2	0.334330	0.349300	0.257602	0.255512
C_3	1.141174	0.306533	0.535923	1.414255
C_4	1.335555	0.585759	0.660533	1.534791
H_5	0.083770	0.162581	0.207033	0.094600
H_6	0.240749	0.303069	0.371543	0.292243
N_7	-0.660181	-0.396664	-0.601210	-0.844255
N_8	-0.911363	-0.524394	-0.563892	-1.058551
F_9	-0.526765	-0.355736	-0.438026	-0.557283
O_{10}	-0.835030	-0.446017	-0.538003	-0.995593
O_{11}	-0.977192	-0.274202	-0.521789	-1.124224
C_{12}	0.597981	0.130683	0.223949	0.652312
C_{13}	0.043928	-0.608786	-0.513265	0.103341
H_{14}	-0.004989	0.151770	0.147757	-0.021008
H_{15}	0.011312	0.175607	0.140515	-0.019916
H_{16}	0.011312	0.175609	0.140516	-0.019915
H_{17}	-0.065997	0.141289	0.149145	-0.032450
H_{18}	-0.066010	0.141284	0.149143	-0.032454

Hydrogen atoms should carry positive charges, consistent with electron withdrawal by neighboring electronegative atoms. At the DFT/Mulliken level, hydrogen charges vary from +0.141289 (H_{18}) to +0.303069 (H_6), while the HF calculations predict values between +0.140515 and +0.371543. However, APT model sometimes calculates negatively the hydrogen atoms. In this context, the APT charges exhibit a broader distribution, ranging from -0.066010 (H_{18}) to +0.597981 (C_{12}-associated environment), indicating the sensitivity of the APT method to local polarization effects and vibrational charge redistribution.

In conclusion, both Mulliken and APT analyses reveal a highly polarized electronic structure for 2-ethoxy-5-fluoro-1H-pyrimidin-4-one. Significant negative charge accumulation is concentrated around the nitrogen, oxygen, and fluorine atoms, whereas positive charge density is primarily localized on selected carbon and hydrogen atoms. This non-uniform charge distribution originates from the combined effects of heteroatom electronegativity, lone-pair electron localization, π-electron delocalization within the pyrimidine ring, and electron-donating contributions from the ethoxy substituent, to be confirmed by simulation analyses. The observed charge anisotropy indicates the presence of efficient intramolecular charge-transfer pathways and provides valuable insight into the molecule's reactivity, intermolecular interactions, hydrogen-bonding capability, and potential electrophilic and nucleophilic attack sites.

3.1. NMR Spectral Analyses of 2-ethoxy-5-fluoro-1H-pyrimidin-4-one Molecule

Nuclear magnetic resonance (NMR) spectroscopy is among the most informative analytical techniques for elucidating molecular structures and probing the electronic environments surrounding carbon and hydrogen nuclei. The chemical shifts observed in both ^{13}C and ^{1}H NMR spectra are highly sensitive to electron density distribution, heteroatom substitution, resonance effects, hydrogen bonding interactions, and intramolecular charge transfer phenomena. Consequently, theoretical NMR calculations provide valuable insights into the electronic structure of heterocyclic compounds and serve as an important complement to experimental spectroscopic investigations (Jeanmairet et al., 2016).

In the present study, the ^{13}C and ^{1}H NMR chemical shifts of 2-ethoxy-5-fluoro-1H-pyrimidin-4-one were calculated using the Gauge-Independent Atomic Orbital (GIAO) approach at the HF/6-31G(d) and B3LYP/6-311+G(2d,p) levels of theory. The calculated isotropic shielding constants were referenced to tetramethylsilane (TMS), and the resulting chemical shift values were compared with available experimental data recorded in $CDCl_3$. The calculated and experimental NMR parameters are summarized in Table 6. The ^{13}C NMR spectrum exhibits significant variations among the carbon atoms owing to the combined effects of the fluorine substituent, carbonyl functionality, ring nitrogen atoms, and ethoxy group. At the B3LYP/6-311+G(2d,p) level, the calculated chemical shifts span from 2.0137 ppm (C_{13}) to 179.845 ppm (C_3), while the HF calculations predict a range between 19.5334 ppm (C_{13}) and 197.365 ppm (C_3). The experimental values lie between 13.98 ppm (C_{13}) and 156.84 ppm (C_3). The most deshielded carbon resonance corresponds to C_3, which is directly influenced by the neighboring electronegative nitrogen atoms and carbonyl functionality within the pyrimidinone ring. Similarly, C_4 and C_2 exhibit large chemical shifts due to their participation in the conjugated heterocyclic framework and their proximity to electron-withdrawing heteroatoms. In contrast, the ethoxy carbon atom C_{13} displays the lowest chemical shift value because of its aliphatic nature and relatively high local electron density. The carbon atom C_{12}, belonging to the ethoxy

substituent, appears in the intermediate region, with calculated values of 53.2954 ppm (B3LYP) and 70.8150 ppm (HF), compared with the experimental value of 63.94 ppm.

A comparison of the computational approaches indicates that the B3LYP/6-311+G(2d,p) method reproduces the experimental ^{13}C NMR trends more accurately than the HF method. The inclusion of electron-correlation effects within the DFT framework leads to a more realistic description of magnetic shielding and electronic delocalization in the heterocyclic ring system. Although some deviations remain for highly deshielded carbon centers, the overall agreement confirms the reliability of the DFT-based calculations.

Table 6. NMR chemical shifts of 2-ethoxy-5-fluoro-1H-pyrimidin-4-one molecule.

Atoms	TMS HF/6-31G(d)	TMS B3LYP/6-311+G(2d,p)	CH_4-HF/6-31G(d)	Exp. in $CDCl_3$
C_3	197.365	179.845	196.479	156.84
C_4	163.133	145.613	162.248	153.66
C_2	159.298	141.778	158.413	145.06
C1	120.514	102.994	119.629	135.16
C_{12}	70.8150	53.2954	62.9298	63.94
C_{13}	19.5334	2.0137	18.6481	13.98
	TMS HF/6-31G(d)	TMS B3LYP/6-311+G(2d,p)	Exp. in $CDCl_3$	
H_6	8.4346	11.5776	12.77	
H_5	7.4795	7.9980	7.828	
H_{17}	4.0261	4.6235	4.324	
H_{18}	3.9617	4.0116		
H_{16}	1.9969	2.2009		
H_{15}	1.8589	2.0116		
H_{14}	1.3332	1.4458	1.298	

The calculated ^1H NMR chemical shifts also show satisfactory agreement with the experimental spectrum. At the B3LYP/6-311+G(2d,p) level, the proton chemical shifts vary between 1.4458 ppm (H_{14}) and 11.5776 ppm (H_6), whereas the HF calculations predict a range from 1.3332 ppm (H14) to 8.4346 ppm (H6). Experimentally observed proton resonances appear at 1.298 ppm (H_{14}), 4.324 ppm (H_{17}), 7.828 ppm (H_5), and 12.77 ppm (H_6). The highest chemical shift is associated with H6, which is attached to the pyrimidinone ring and experiences strong deshielding due to the neighboring nitrogen and carbonyl groups, as well as possible intermolecular hydrogen-bonding interactions. The aromatic proton H_5 also resonates downfield owing to the electron-withdrawing influence of the fluorine substituent and the heterocyclic ring system. Conversely, the protons belonging to the ethoxy group (H_{14}-H_{18}) appear at lower chemical shifts, showing their relatively electron-rich aliphatic environment.

The overall agreement between the calculated and experimental ^1H NMR data confirms that the electronic structure of 2-ethoxy-5-fluoro-1H-pyrimidin-4-one is well described by the applied quantum-chemical models. In particular, the DFT-based GIAO calculations reproduce the experimental trends more successfully than the HF approach, highlighting the importance of electron-correlation effects in accurately predicting magnetic shielding constants.

In summary, the theoretical NMR investigation supports the proposed molecular structure of 2-ethoxy-5-fluoro-1H-pyrimidin-4-one and provides detailed information regarding the influence of fluorine substitution, heteroatom incorporation, and π-electron delocalization on the local magnetic environments of carbon and hydrogen nuclei. The close agreement between the experimental and calculated chemical shifts further confirms the validity of the optimized molecular geometry and the reliability of the computational methodology employed throughout this study.

3.4 Frontier Molecular Orbital Analysis of 2-ethoxy-5-fluoro-1H-pyrimidin-4-one

Frontier molecular orbital (FMO) analysis is an effective approach for understanding the electronic structure, charge-transfer characteristics, and chemical reactivity of molecular systems. In the present study, the highest occupied molecular orbital (HOMO) and lowest unoccupied molecular orbital (LUMO) of 2-ethoxy-5-fluoro-1H-pyrimidin-4-one were investigated to elucidate the electronic behavior of the molecule. The HOMO is associated with the electron-donating capability of the system, whereas the LUMO represents its electron-accepting tendency (Fig. 4). Consequently, the HOMO–LUMO energy gap (ΔE) serves as an important descriptor of molecular stability, charge-transfer efficiency, electronic excitation, and chemical reactivity. In general, molecules with smaller energy gaps exhibit higher polarizability and reactivity, while larger gaps are indicative of greater kinetic stability.

a) b)

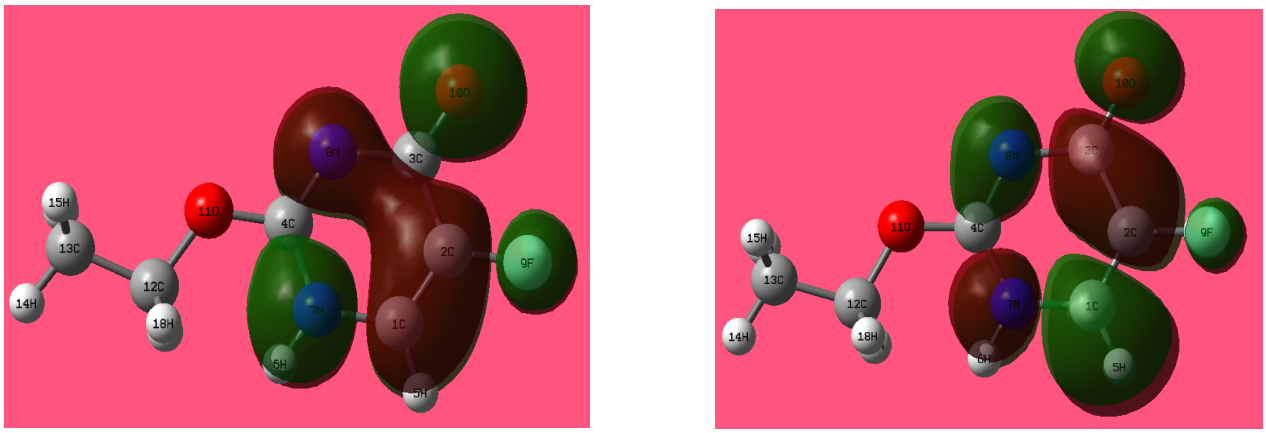

Figure 4.3D spatial distributions of **a-**HOMO and **b-**LUMO orbitals of 2-ethoxy-5-fluoro-1H-pyrimidin-4-one.

The calculated frontier orbital energies at the DFT/B3LYP/6-31+G(d,p) and HF/6-31+G(d,p) levels provide valuable information regarding the electronic nature of the title compound. The obtained HOMO-LUMO gap indicates that 2-ethoxy-5-fluoro-1H-pyrimidin-4-one possesses a favorable balance between structural stability and electronic responsiveness (Punchkovska & Kostyukevych, 2002). Such a characteristic is particularly important for heterocyclic compounds containing multiple electronegative atoms, where charge redistribution and orbital interactions play significant roles in determining physicochemical properties.

The three-dimensional (3D) orbital distributions reveal that the HOMO is predominantly localized over the pyrimidinone ring, especially around the nitrogen atoms, carbonyl oxygen atom, and the conjugated π-electron framework. The presence of lone-pair electrons on the heteroatoms contributes significantly to the

HOMO density, indicating that these regions may act as electron-donating centers during intermolecular interactions. In contrast, the LUMO is mainly distributed over the pyrimidinone skeleton and carbonyl-containing region, extending partially toward the fluorine-substituted carbon atom. This distribution shows that electron acceptance preferentially occurs within the heterocyclic ring system, where the electron-withdrawing effects of the fluorine and carbonyl groups stabilize the incoming electron density.

The observed separation between the HOMO and LUMO regions indicates the possibility of ICT within the molecule. Upon electronic excitation, electron density is expected to migrate from the electron-rich heterocyclic and ethoxy-containing regions toward the more electron-deficient carbonyl- and fluorine-influenced portions of the pyrimidine ring. This charge-transfer process contributes to the optical and electronic properties of the molecule and is consistent with the electronic transitions observed in the UV-Vis absorption spectra.

Table 7. Calculated energies of 2-ethoxy-5-fluoro-1H-pyrimidin-4-one molecule in ground state with singlet symmetry at B3LYP/6-31+G(d,p) basis set.

Quantities	**Values**
Lowest MO Eigen value (a.u.)	-24.73744
Highest MO Eigen value (a.u.)	6.354210
HOMO (a.u.)	-0.25500
LUMO (a.u.)	-0.04667
HOMO–LUMO gap (a.u.), $\|\Delta E\|$	0.208400
χ (Electronegativity) (a.u.), [IP + EA]/2	0.150835
μ, Chemical potential, $-$[IP + EA]/2	-0.150835
η (Chemical hardness) (a.u.) [IP − EA]/2	0.104200
ζ (Softness) (a.u.)$^{-1}$, 1/2η	4.798464
ψ (Electrophilicity index) (a.u.), $\mu^2/2\eta$	0.109171
Maximum charge transfer index (ΔN_{max}=-μ/η)	1.447553

In addition to the frontier orbital energies, several global reactivity descriptors can be derived from the HOMO and LUMO values, including IP, EA, η, S, χ, μ, and ω parameters, which provide quantitative information regarding the molecule's tendency to donate or accept electrons and its overall chemical reactivity. The calculated descriptors indicate that the title compound possesses moderate chemical hardness and appreciable softness, reflecting a balanced electronic structure capable of participating in both electrophilic and nucleophilic processes. Furthermore, the relatively high electronegativity arising from the fluorine, nitrogen, and oxygen atoms enhances the electron-withdrawing character of the molecule and contributes to its electronic stabilization.

To further quantify the electronic behavior, global reactivity descriptors were derived from the FMO energies (Table 7). The calculated values for electronegativity (0.150835 a.u.), chemical hardness (0.104200 a.u.), chemical softness (0.104200 a.u.), chemical potential (-0.150835 a.u.), *maximum charge transfer index (*1.447553*),* and the electrophilicity index (0.109171 a.u.) reveal moderate hardness and appreciable softness. This structural balance displays that the molecule is capable of engaging in both nucleophilic and electrophilic interactions.

To conclude, the FMO analysis demonstrates that 2-ethoxy-5-fluoro-1H-pyrimidin-4-one exhibits a highly polarized electronic structure governed by the combined effects of the pyrimidinone ring, fluorine substituent, carbonyl group, and ethoxy functionality. The distribution of the frontier orbitals highlights the important role of heteroatoms in controlling electron density and charge-transfer pathways. The mentioned findings provide a deeper understanding of the molecule's reactivity, stability, spectroscopic behavior, and potential utility in pharmaceutical, agrochemical, and functional-material applications.

3.5 Electrostatic Potential and Molecular Electrostatic Potential Analysis of 2-Ethoxy-5-Fluoro-1H-pyrimidin-4-one

To gain deeper information about the electronic distribution and reactive sites of 2-ethoxy-5-fluoro-1H-pyrimidin-4-one compound, electrostatic potential (ESP) and molecular electrostatic potential (MEP) surfaces were generated at the B3LYP/6-31+G(d,p) level of theory. These surface maps provide a visual representation of the electron-density distribution throughout the molecule and facilitate the identification of regions susceptible to electrophilic and nucleophilic interactions. In addition, ESP and MEP analyses are valuable tools for predicting intermolecular interactions, hydrogen-bonding behavior, molecular recognition processes, and the preferred sites of chemical reactivity.

The simulated ESP map image given in Fig. 5 reveals a highly non-uniform charge distribution arising from the presence of electronegative fluorine, oxygen, and nitrogen atoms within the molecular structure. The most negative electrostatic potential regions are predominantly concentrated around the carbonyl oxygen atom and the ring nitrogen atoms of the pyrimidinone moiety. The electron-rich centers exhibit a strong tendency toward electrophilic attack and may serve as favorable hydrogen-bond acceptor sites. The fluorine atom also contributes to the negative electrostatic potential due to its high electronegativity, although its contribution is generally less pronounced than that of the carbonyl oxygen atom.

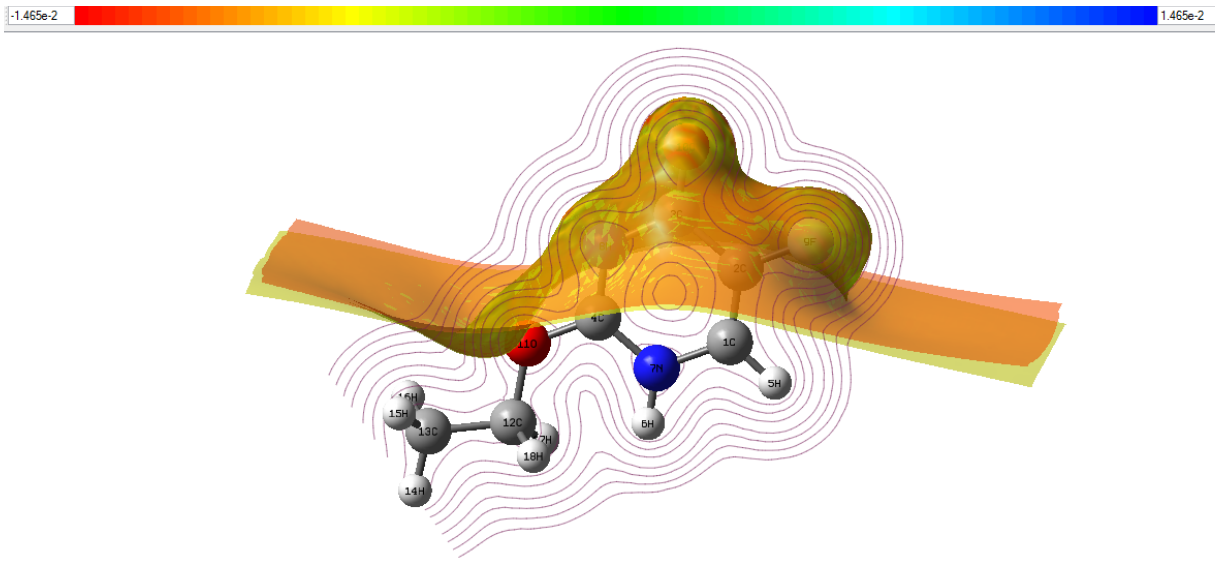

Figure 5. 3D plot for ESP map for 2-ethoxy-5-fluoro-1H-pyrimidin-4-one molecule

The 3D MEP surface shown in Fig. 6 further highlights the distribution of positive and negative electrostatic potential over the molecular structure of 2-ethoxy-5-fluoro-1H-pyrimidin-4-one molecule. The regions represented by red and yellow colors correspond to areas of high electron density and negative potential,

which are mainly localized around the carbonyl oxygen atom, fluorine substituent, and ring nitrogen atoms. The reported regions are expected to participate actively in intermolecular interactions involving electrophilic species. In contrast, the positive electrostatic potential regions, typically represented by blue colors, are primarily located around the hydrogen atoms of the N–H group and the ethoxy substituent. These electron-deficient regions may act as hydrogen-bond donors and are favorable sites for nucleophilic interactions.

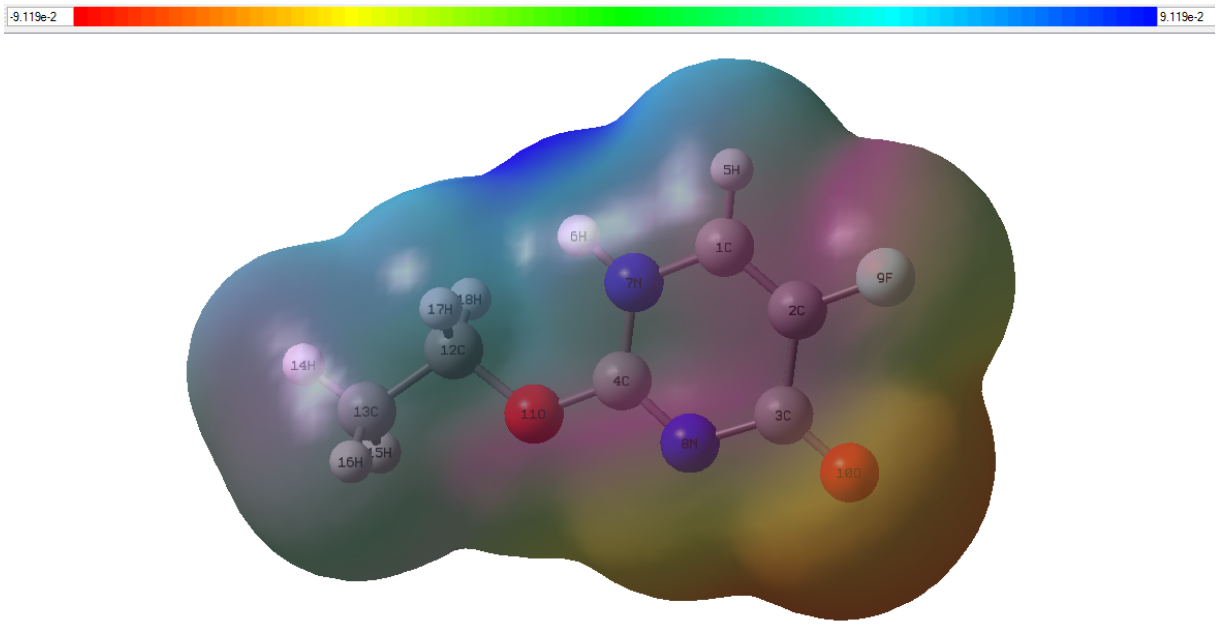

Figure 6. 3D plots of MEP image of 2-ethoxy-5-fluoro-1H-pyrimidin-4-one molecule

The intermediate potential regions distributed throughout the pyrimidinone ring indicate significant electron delocalization within the heterocyclic structure. The conjugative interaction among the carbonyl group, nitrogen atoms, fluorine substituent, and the π-electron system contributes to a balanced redistribution of electron density across the molecule. Such delocalization plays a crucial role in stabilizing the molecular structure and influences both its spectroscopic and reactive properties.

The coexistence of well-defined electron-rich and electron-deficient regions demonstrates the polarized nature of 2-ethoxy-5-fluoro-1H-pyrimidin-4-one compound. This polarization originates from the combined electron-withdrawing effects of the fluorine atom and carbonyl group, together with the electron-donating contribution of the ethoxy substituent. As a result, the molecule studied in the present work possesses multiple active sites capable of participating in various non-covalent interactions, including hydrogen bonding, dipole-dipole interactions, electrostatic attractions, and charge-transfer processes (Zhang et al.,2016).

When considered alongside the frontier molecular orbital and UV-Vis analyses, the ESP and MEP results provide strong evidence for intramolecular charge redistribution within the molecule. The pronounced electronic polarization and favorable charge-transfer characteristics suggest that 2-ethoxy-5-fluoro-1H-pyrimidin-4-one possesses desirable electronic properties that may be relevant to its chemical reactivity, biological activity, molecular recognition capability, and potential applications in pharmaceutical and functional-material research.

4. Conclusion

In the present study, a detailed quantum-chemical investigation of 2-ethoxy-5-fluoro-1H-pyrimidin-4-one was performed using DFT/B3LYP and HF computational approaches in order to examine its molecular structure, NMR characteristics, atomic charge distribution, thermochemical behavior, electronic properties, and reactivity descriptors. Geometry optimization confirmed the stability of the heterocyclic pyrimidinone structure and displayed that the fluorine substituent, carbonyl functionality, and ethoxy group collectively influence the molecular electronic environment. The optimized structural parameters obtained from both theoretical methods exhibited good consistency, supporting the reliability of the computational methodology. Moreover, theoretical ^{1}H and ^{13}C NMR analyses performed using the GIAO formalism successfully reproduced the experimental spectral trends. The B3LYP calculations provided closer agreement with the experimental chemical shifts than the HF quantum computational method, emphasizing the critical role of electron-correlation effects in accurately describing magnetic shielding environments. The observed chemical-shift distribution confirmed the strong deshielding influence of the fluorine atom, carbonyl group, and ring nitrogen atoms on adjacent nuclei.

Mulliken and APT atomic charge analyses also revealed significant electronic polarization within the molecule. The carbonyl oxygen atom, fluorine substituent, and pyrimidine nitrogen atoms were identified as the principal electron-rich centers, whereas several carbon and hydrogen atoms carried positive charges. Although the absolute charge magnitudes differed between the Mulliken and APT approaches, both methods consistently described the same qualitative charge-distribution pattern, confirming substantial intramolecular charge redistribution throughout the molecular structure.

Further, the thermochemical calculations indicated that the molecule possesses favorable energetic stability and a relatively polar character. Frontier molecular orbital analysis showed that the HOMO is primarily associated with the heteroatom-rich pyrimidinone ring, while the LUMO is concentrated in the carbonyl- and fluorine-influenced regions of the molecule. The resulting HOMO-LUMO separation facilitates intramolecular charge transfer and contributes significantly to the electronic and optical behavior of the compound. Global reactivity descriptors further indicated moderate chemical hardness together with appreciable softness, revealing that the molecule can participate in both electrophilic and nucleophilic interactions.

The simulated UV-Vis absorption spectrum revealed that the principal electronic transitions originate from $\pi \rightarrow \pi^*$ and $n \rightarrow \pi^*$ excitations involving the conjugated heterocyclic system and heteroatom lone pairs. In addition, ESP and MEP surface analyses identified the carbonyl oxygen atom, fluorine atom, and pyrimidine nitrogen atoms as the most favorable sites for electrophilic interactions, whereas the N-H and ethoxy hydrogen atoms constitute the principal positive-potential regions capable of participating in hydrogen-bonding and nucleophilic interactions.

In summary, the combined structural, spectroscopic, thermochemical, and electronic analyses establish that 2-ethoxy-5-fluoro-1H-pyrimidin-4-one possesses a stable and highly polarized donor–acceptor electronic structure characterized by efficient charge redistribution, well-defined reactive regions, and favorable electronic-response characteristics. The findings obtained from the present study provide a reliable theoretical foundation for future experimental investigations and indicate that this fluorinated pyrimidinone

derivative may be a promising candidate for pharmaceutical, agrochemical, and advanced functional-material applications.

References

Antony, J., & Grimme, S. (2006). Density functional theory including dispersion corrections for intermolecular interactions in a large benchmark set of biologically relevant molecules. Physical Chemistry Chemical Physics, 8(45), 5287–5293.

Bayrakdar, A., Nivetha, G. F., Demircali, A., Kizak, H., Tasli, P. T., Yıldırım, F., ... & Smerat, A. (2026). Synthesis of new pyrazolo pyrimidine disazo dyes, theoretical and experimental comparison of their characteristic properties and in silico prediction of their possible antibacterial activity. Journal of Computational Biophysics and Chemistry, 1–27.

Becke, A. D. (1993). Density-functional thermochemistry. III. The role of exact exchange. The Journal of Chemical Physics, 98(7), 5648–5652.

Boo, B. H., Cho, H., & Kang, D. E. (2007). Ab initio and DFT investigation of structures and energies of low-lying isomers of ZnxSex (x= 1–4) clusters. Journal of Molecular Structure: THEOCHEM, 806(1-3), 77–83.

Brown, D. J., Ellman, J. A., & Taylor, E. C. (2000). The Pyridazines, Volume 57, Supplement 1. John Wiley & Sons.

Buyukuslu, H., Akdogan, M., Yildirim, G., & Parlak, C. (2010). Ab initio Hartree-Fock and density functional theory study on characterization of 3-(5-methylthiazol-2-yldiazenyl)-2-phenyl-1H-indole. Spectrochimica Acta Part A: Molecular and Biomolecular Spectroscopy, 75(4), 1362–1369.

Cyrański, M. K. (2005). Energetic aspects of cyclic pi-electron delocalization: evaluation of the methods of estimating aromatic stabilization energies. Chemical Reviews, 105(10), 3773–3811.

Dennington II, R., Keith, T., & Millam, J. (2007). GaussView, Version 4.1.2. Semichem, Inc.

Fanchini, G., Tagliaferro, A., Conway, N. M. J., & Godet, C. (2002). Role of lone-pair interactions and local disorder in determining the interdependency of optical constants of a− C N: H thin films. Physical Review B, 66(19), 195415.

Francl, M. M., Pietro, W. J., Hehre, W. J., Binkley, J. S., Gordon, M. S., DeFrees, D. J., & Pople, J. A. (1982). Self-consistent molecular orbital methods. XXIII. A polarization-type basis set for second-row elements. The Journal of Chemical Physics, 77(7), 3654–3665.
Frisch, M. J., et al. (2009). Gaussian 09, Revision A.02. Gaussian, Inc.

Furer, V. L., Potapova, L. I., & Kovalenko, V. I. (2017). DFT study of hydrogen bonding and IR spectra of calix [6] arene. Journal of Molecular Structure, 1128, 439–447.

Gökce, H., & Bahçeli, S. (2025). Biological evaluation, spectroscopic characterization and DFT computations of an oxalamide derivative (BFMO). Journal of Molecular Structure, 143654.

Gökce, H., Bahceli, S., & Alpaslan, G. (2024). Structural, vibrational, electronic, NLO and molecular docking analyses of two novel Cu (II) and Pd (II) complexes with pyridine and oxadiazole coordination. Inorganic Chemistry Communications, 168, 112852.

Hsu, C. Y., Abdulazez, A. A., Priya, G. P., Ray, S., Pal, A., Yusupov, Y., ... & Alkhathami, A. G. (2026). Pt decorated BN nanocage as an effective sensor material for the detection of 5-Fluorouracil anticancer drug. Materials Chemistry and Physics, 132204.

Hughes, R. P., & O'Hagan, D. (2010). Graphical Abstracts/J. Fluorine Chem. 131 (2010) 1049–1056. Journal of Fluorine Chemistry, 131, 1049–1056.

Ibrahim, A., El Aal, M. A., El-Zahed, H., & Mabied, A. F. (2026). DFT study on tunable electronic and adsorption properties of poly (vinyl alcohol)/copper oxide/graphene oxide hybrid nanostructures. Scientific Reports, 16(1), 16191.

Jeanmairet, G., Levy, N., Levesque, M., & Borgis, D. (2016). Molecular density functional theory of water including density–polarization coupling. Journal of Physics: Condensed Matter, 28(24), 244005.

Joule, J. A., & Mills, K. (2012). Heterocyclic chemistry at a glance. John Wiley & Sons.

Jumabaev, A., Koyambo-Konzapa, S. J., Hushvaktov, H., Absanov, A., Khudaykulov, B., Holikulov, U., ... & Nsangou, M. (2024). Intermolecular interactions in water and ethanol solution of ethyl acetate: Raman, DFT, MEP, FMO, AIM, NCI-RDG, ELF, and LOL analyses. Journal of Molecular Modeling, 30(10), 349.

Katritzky, A. R., Ramsden, C. A., Joule, J. A., & Zhdankin, V. V. (2010). Handbook of heterocyclic chemistry. Elsevier.

Kawamura, S., & Sanemitsu, Y. (1993). A novel ring transformation of oxazinones and azetidinones into pyrimidinones. The Journal of Organic Chemistry, 58(2), 414–418.

Koopmans, T. (1934). Über die Zuordnung von Wellenfunktionen und Eigenwerten zu den einzelnen Elektronen eines Atoms. Physica, 1(1-6), 104–113.

Laury, M. L., Carlson, M. J., & Wilson, A. K. (2012). Vibrational frequency scale factors for density functional theory and the polarization consistent basis sets. Journal of Computational Chemistry, 33(30), 2380–2387.

Lee, C., Yang, W., & Parr, R. G. (1988). Development of the Colle-Salvetti correlation-energy formula into a functional of the electron density. Physical Review B, 37(2), 785.

Meanwell, N. A. (2018). Fluorine and fluorinated motifs in the design and application of bioisosteres for drug design. Journal of Medicinal Chemistry, 61(14), 5822–5880.

Mohammadi, M. D., Abdullah, H. Y., Qadir, K. W., & Suvitha, A. (2023). Theoretical investigation of intermolecular interactions between CNT, SiCNT and SiCGeNT nanomaterials with vinyl chloride molecule: a DFT, NBO, NCI, and QTAIM study. Diamond and Related Materials, 131, 109602.

Muthuraman, M., Le Fur, Y., Bagieu-Beucher, M., Masse, R., Nicoud, J. F., George, S., ... & Desiraju, G. R. (2000). C–H⋯ O and C–H⋯ N hydrogen bond networks in the crystal structures of some 1, 2-dihydro-N-aryl-4, 6-dimethylpyrimidin-2-ones. Journal of Solid State Chemistry, 152(1), 221–228.

Nangia, A. (2006). Supramolecular synthesis of 1D chains and 2D layers in hydrogen bond networks of ureas and 2-pyrimidinones. Topics in Stereochemistry, 25, 135–176.

Noser, A. A., Khalifa, M. M., Salman, I. N., & Salem, M. M. (2026). Advanced pyrimidinone chemistry: a comprehensive review of synthetic pathways and biological potency. Chemical Papers, 1–23.

Palusiak, M., & Krygowski, T. M. (2007). Application of AIM parameters at ring critical points for estimation of π-electron delocalization in six-membered aromatic and quasi-aromatic rings. Chemistry–A European Journal, 13(28), 7996–8006.

Parlak, C., Akdogan, M., Yildirim, G., Karagoz, N., Budak, E., & Terzioglu, C. (2011). Density functional theory study on the identification of 3-[(2-morpholinoethylimino) methyl] benzene-1, 2-diol. Spectrochimica Acta Part A: Molecular and Biomolecular Spectroscopy, 79(1), 263–271.

Parr, R. G. (1989). Density functional theory of atoms and molecules. In Horizons of Quantum Chemistry: Proceedings of the Third International Congress of Quantum Chemistry Held at Kyoto, Japan, October 29-November 3, 1979 (ss. 5-15). Springer Netherlands.

Puchkovska, G. O., & Kostyukevych, S. (Eds.). (2002). Spectroscopy of Molecules and Crystals. SPIE.

Purser, S., Moore, P. R., Swallow, S., & Gouverneur, V. (2008). Fluorine in medicinal chemistry. Chemical Society Reviews, 37(2), 320–330.

Sharma, A. K., Jayakumar, S., Hundal, M. S., & Mahajan, M. P. (2002). Tandem sigmatropic shifts in [4+ 2] cycloaddition reactions of 1, 3-diazabuta-1, 3-dienes with butadienylketene: synthesis of pyrimidinone derivatives. Journal of the Chemical Society, Perkin Transactions 1, (6), 774–784.

Sivaraman, B., Maji, L., Chagaleti, B. K., & Muthukumaradoss, K. (2026). Exploration of a novel imidazo [4, 5-b] pyridine–dihydropyrimidinone hybrids as aurora kinase a inhibitors: integrated pharmacophore modelling, docking and simulation approaches. Molecular Diversity, 1–22.

Snyder, J. P., & Carlsen, L. (1977). Lone pair-lone pair interactions in unsymmetrical systems: RSSR vs. RSOR. Journal of the American Chemical Society, 99(9), 2931–2942.

Sobczyk, L., Grabowski, S. J., & Krygowski, T. M. (2005). Interrelation between H-bond and pi-electron delocalization. Chemical Reviews, 105(10), 3513–3560.

Steinmann, S. N., Mo, Y., & Corminboeuf, C. (2011). How do electron localization functions describe π-electron delocalization?. Physical Chemistry Chemical Physics, 13(46), 20584–20592.

Stephens, P. J., Devlin, F. J., Chabalowski, C. F., & Frisch, M. J. (1994). Ab initio calculation of vibrational circular dichroism spectra using density functional force fields. The Journal of Physical Chemistry, 98(45), 11623–11627.

Tortorella, S., Talamo, M. M., Cardone, A., Pastore, M., & De Angelis, F. (2016). Benchmarking DFT and semi-empirical methods for a reliable and cost-efficient computational screening of benzofulvene derivatives as donor materials for small-molecule organic solar cells. Journal of Physics: Condensed Matter, 28(7), 074005.

Tsuzuki, S., & Uchimaru, T. (2020). Accuracy of intermolecular interaction energies, particularly those of hetero-atom containing molecules obtained by DFT calculations with Grimme's D2, D3 and D3BJ dispersion corrections. Physical Chemistry Chemical Physics, 22(39), 22508–22519.

Wolff, S. K., & Ziegler, T. (1998). Calculation of DFT-GIAO NMR shifts with the inclusion of spin-orbit coupling. The Journal of Chemical Physics, 109(3), 895–905.

Xiao, J., Zhao, Y. P., Fan, X., Cao, J. P., Kang, G. J., Zhao, W., & Wei, X. Y. (2017). Hydrogen bonding interactions between the organic oxygen/nitrogen monomers of lignite and water molecules: A DFT and AIM study. Fuel Processing Technology, 168, 58–64.

Xu, Y., Hao, J., Ju, H., He, S., Wang, J., Jia, C., & Guo, X. (2024). Identifying π–π and π–lone pair interactions in a single-molecule junction. ACS Materials Letters, 6(5), 1961–1967.

Young, D. C. (2001). Computational chemistry: A practical guide for applying techniques to real world problems. John Wiley & Sons Inc.

Zhang, Y., Luo, Y., Zhang, Y., Yu, Y. J., Kuang, Y. M., Zhang, L., ... & Hou, J. G. (2016). Visualizing coherent intermolecular dipole–dipole coupling in real space. Nature, 531(7596), 623–627.

Zhou, W., & Umezawa, N. (2015). Band gap engineering of bulk and nanosheet SnO: an insight into the interlayer Sn–Sn lone pair interactions. Physical Chemistry Chemical Physics, 17(27), 17816–17820.

BEYANLAR / DECLARATIONS

SECTION	STATEMENT / DISCLOSURE
Yazar Katkıları ***Author Contributions***	**Yazar Katkıları:** GK, UE, GY ve MBT proje fikrini geliştirmiş ve hesaplamaları tasarlamıştır. GK, UE ve GY metodoloji, proje yönetimi ve araştırmanın yanı sıra malzeme üretimini gerçekleştirmiştir. UE, GY ve MBT ise teorik kurgu ve kaynak sağlama, biçimsel analiz ile gözden geçirme ve düzenleme işlemlerini yürütmüştür **Author contributions:** GK, UE, GY and MBT conceived the idea for the project and designed the calculations. GK, UE and GY performed methodology, project administration, investigation also performed materials production. UE and GY and MBT performed theoretical set-up and resources, formal analysis, review & editing.
Çıkar Çatışması: ***Conflict of Interest***	Yazarlar, bu makalede sunulan çalışmayı etkilediği izlenimi yaratabilecek bilinen hiçbir rekabetçi finansal çıkar veya kişisel ilişki bulunmadığını beyan ederler. The authors declare that they have no known competing financial interests or personal relationships that could have appeared to influence the work reported in this paper.
Finansman ***Funding***	Bu araştırma kamuya ait, ticari veya kâr amacı gütmeyen sektörlerdeki hiçbir fon sağlayıcı kuruluştan özel bir destek veya hibe almamıştır. This research received no specific grant from any funding agency in the public, commercial, or not-for-profit sectors.
Üretken Yapay Zekâ Beyanı ***Declaration of Generative AI***	
Etik Kurul Onayı ***Ethics Approval***	
Teşekkür ***Acknowledgements***	-